MODE II DELAMINATION FATIGUE CRACK GROWTH CHARACTERISTICS OF GFRP LAMINATES WITH WASTE GFRP MILLED CHIPS INTERLEAF

H. Yokogawa[1*], Y. Aono[1], H. Noguchi[1]

[1]*Department of Mechanical Engineering, Kyushu University,*
Solid Mechanics Laboratory, 744 Motooka, Nishi-ku, Fukuoka, 819-0395, Japan
**h.yokogawa.054@s.kyushu-u.ac.jp*

Keywords: GFRP, Fatigue crack propagation, Mode II, Recycling

Abstract

In this study, we investigated the mode II delamination fatigue crack growth characteristics of GFRP laminates with a waste GFRP milled chip interleaf for recycling waste GFRP. We used a recycle method investigated in a previous study. End-notched flexure fatigue tests were conducted with GFRP laminates with the interleaf and UD laminates under four types of maximum test loads with P_{max} = 0.69, 0.59, 0.49, and 0.44 kN. In addition, we observed fatigue damage during tests and fracture surfaces. We found that the fatigue characteristics could be divided into three regions according to the load levels. In the case of P_{max} = 0.44 kN, the crack in the GFRP laminates with the interleaf did not propagate, whereas the crack in the normal UD laminates grew to failure under the same test load. This result indicated that the interleaf was effective in impeding mode II delamination fatigue crack growth.

1 Introduction

Fiber-reinforced plastics (FRPs) have been used in various structures because their specific strength and stiffness are higher than those of other materials. The amount of waste FRP has increased with this increased usage and has reached 400,000 tons per years in Japan. Most of this is disposed off in landfills or is incinerated. Only a small amount of the waste is being used as fuel for concrete production. Disposal involves problems such as a shortage of final disposal sites, the non-biodegradability of FRPs, etc.

In a previous study, we devised a recycling method for waste glass-fiber-reinforced plastic (GFRP) to reuse milled waste GFRP as an interlaminar reinforcement because the interlaminar strength of normal FRP laminates is low [1]. The delamination of FRP laminates significantly weakens the composite structure. We manufactured GFRP laminates with an interleaf of waste GFRP chips and normal laminates. Lee et al. [2] referred to composites with interleaves as hybrid composites, and we followed that convention (hereinafter we refer to GFRP laminates with the chip interleaf as hybrid laminates). Static tests on these laminates were carried out, and the bridging effect and shear support by the chip interleaf were observed. The investigation of mode II fatigue characteristics of FRP laminates is important, and some studies have been conducted to examine mode II fatigue characteristics [3-6]. However, no study has been conducted on laminates with an interleaf of waste GFRP chips because the tensile strength of composites made from waste GFRP chips is very low. Hence, in this study,

we carried out end-notched flexure (ENF) fatigue tests to examine the mode II delamination fatigue crack growth characteristics of hybrid and normal laminates.

2 Experimental methods

2.1 Materials and specimens

GFRP laminates were fabricated by vacuum-assisted resin transfer molding (VaRTM). The fabrics used were unidirectional (UD) glass fibers by SARTEX, which consisted of 0° at 94.6%, 90° at 4.4%, and stitch at 1.0%. Spa MV-5000 vinyl ester resin by Ishikawa Ink was used as the matrix. Waste bathtubs made of GFRP were used for material recycling. The bathtubs were milled using a rolling mill from Rasa Industries. Then, we used an atomizer from Tokyo Atomizer. The chips obtained by milling the waste GFRP were used for making the interleaves. Figure 1 shows the concept of the interlayer hybrid GFRP. Table 1 lists the mechanical properties of the normal and hybrid laminates. Here, the characters "0, //" and the subscripted "3" in Table 1 imply a 0° fiber layer, the chip interleaf, and the number of lamination layers, respectively.

We modeled $[0_{10}]$ as normal laminates and $[0_5//0_5]$ as hybrid laminates. Figures 2 and 3 show the lamina configuration and specimen configuration. Hybrid specimens were about 1.0 mm thicker than normal ones. Each specimen contained a Teflon film folded in half for a delamination starter. The Teflon film was located mid-plane. The shaded portion in Fig. 2 indicates the area that contains the Teflon film. The crack length *a* in Fig. 3 is defined as the length from a test jig supporting point to a crack tip. Pre-cracks were started with a thin cutter. The pre-crack length *a* for each specimen was about 27 mm. We cut specimens from the center of the laminates because the fringe area of the laminates was unstable. A band-saw was used to cut the laminates.

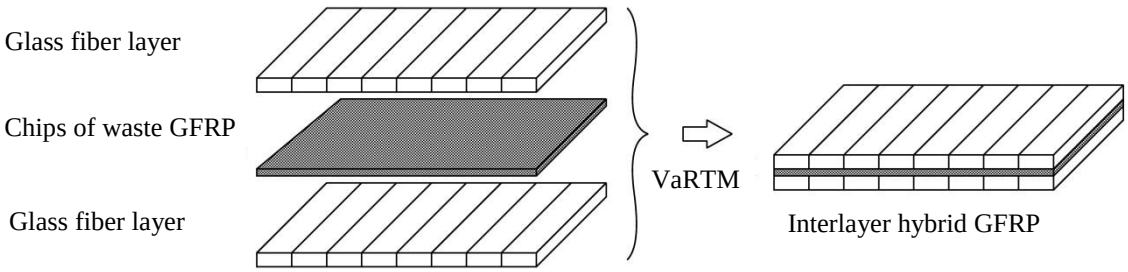

Figure 1. Concept of interlayer hybrid GFRP.

Material	E_1 [Gpa]	v_{12}	E_2 [Gpa]	G_{12} [Gpa]
$[0_3]$	31.4	0.29	14.6	3.78
[0//0//0]	24.3	0.26	8.37	3.32

(a)

	$[0_3]$	[0//0//0]	$[90_3]$	[90//90//90]
σ_B [MPa]	736	605	29.1	31.2
σ_B / ρ [km]	42.3	38.3	1.67	1.98

σ_B: Ultimate strength, ρ: density.

(b)

Table 1. Mechanical properties: (a) Elastic moduli; (b) Tensile strength.

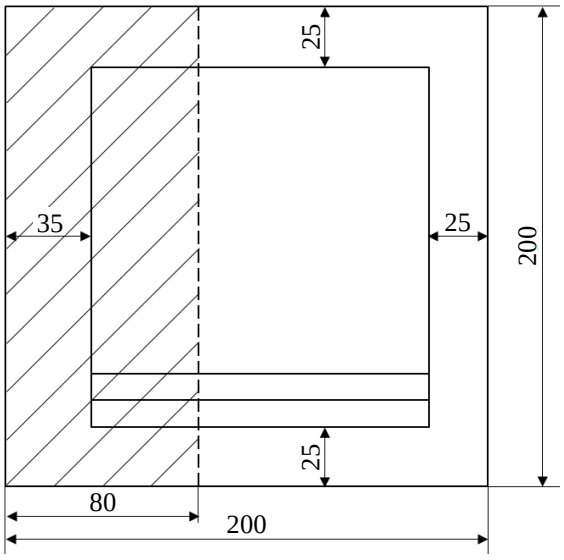

Figure 2. Lamina configuration [mm]

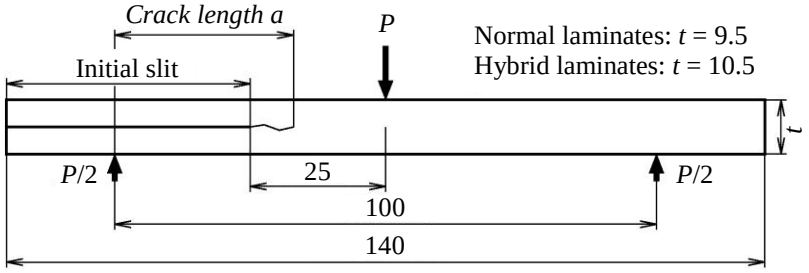

Figure 3. Specimen configuration [mm]

2.2 ENF fatigue test

The testing machine used was a Shimadzu Servo Pulsar, which has a 10-kN load capacity. We conducted fixed-amplitude load fatigue tests with hybrid and normal specimens at a frequency of 5 Hz. The fatigue test was conducted under load control at a stress ratio R = 0.1 in room-temperature air. The maximum test loads were P_{max} = 0.69, 0.59, 0.49, and 0.44 kN.

Hybrid specimens with the chip interleaf on the pre-crack were placed on the testing machine as shown in Fig. 4(a). However, in the test with P_{max} = 0.44 kN, we used the reversed setting shown in Fig. 4(b) because the crack growth behavior in the usual setting was different from that with the other maximum loads. In addition, Fig. 4 shows the model of the crack growth behavior of hybrid specimens. For the usual setting, the fatigue crack grew at an angle of about 45° from horizontal towards the upper-side interface between the chip interleaf and the fiber layer, then along the interface as shown in Fig. 4(a). Figure 4(b) shows the crack growth behavior for the reversed setting. A crack in normal specimens grew along the interlaminar of the pre-crack position.

We regarded the specimen as a failure when the crack length was extended to a = 50 mm. We appropriately stopped the testing machine during the test and recorded surfaces of specimen sides with the plastic replica technique to observe the fatigue damage and to measure the crack length. An optical microscope was used to measure the crack length and observe the sides and the fracture surface.

The energy release rate was calculated in compliance with the annex of JIS K7086-2. The compliance was calculated by the method of least squares using the test load and loading point displacement values that were recorded in the test.

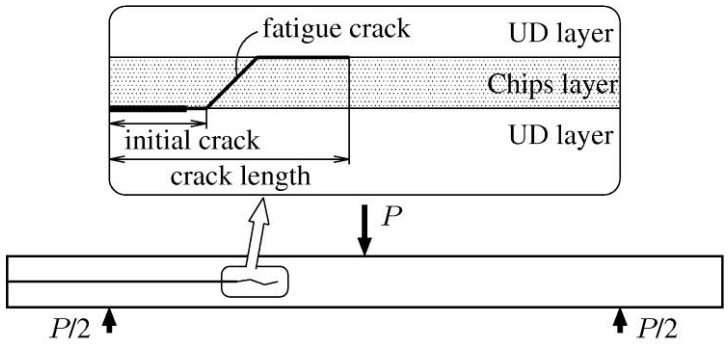

(a)

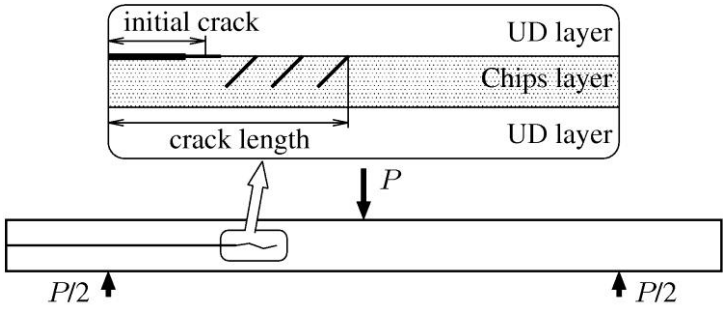

(b)

Figure 4. Position of initial crack and crack growth behavior of hybrid specimens in: (a) usual setting; (b) reverse setting.

3 Experimental results

Figure 5 shows the relation between the crack growth rate da/dN and the energy release rate range ΔG_{II} (in the graphs, hereafter, the hybrid laminates, normal laminates, and hybrid laminates in the reversed setting are referred to as hybrid, normal, and r-hybrid, respectively). The crack growth rate was calculated using the average of crack lengths after a number of cycles. In the case of $\Delta G_{II} > 600$ J/m^2, the relation was approximately expressed by a straight line without regarding the existence of the chip interleaf. Meanwhile, in the case of $\Delta G_{II} \leq 600$ J/m^2, the relation was scattered and expressed by various straight lines. We describe the results in three regions. The first is a higher load region for $\Delta G_{II} > 600$ J/m^2, the second is a medium load region for $\Delta G_{II} \leq 600$ J/m^2, and the third is a non-propagating crack region.

Figure 6 shows the relation between the crack length a and the number of cycles N. All graphs have two crack lengths because we measured crack lengths on both sides of the specimen.

The relation between the hybrid and the normal specimen was the same with $P_{max} = 0.69$ kN, which was in the higher load region. The fatigue crack grew between the interleaf and the UD layer in the hybrid specimen. Moreover, the fatigue crack grew between the UD layers in the normal laminates. The presence of the interleaf appeared to not affect the crack growth rate when the test load was relatively high.

Next, the medium load region is described. The number of cycles to failure of the hybrid specimen was about three times more than that of the normal specimen with $P_{max} = 0.59$ kN. Conversely, the number of cycles to failure of the normal specimen was about eight times more than that of the hybrid specimen for $P_{max} = 0.49$ kN. This scattering will be discussed in the next section.

The crack in the hybrid specimen was arrested at $N = 2.5 \times 10^6$ with $P_{max} = 0.44$ kN. The crack, which stayed in the interleaf, did not propagate to the interface between the chip interleaf and the UD layer. Accordingly, we raised the test load from $P_{max} = 0.44$ kN to 0.49 kN until the crack reached the interface. The crack grew to the interface at $N = 3.1 \times 10^6$, so

we decreased the test load back to P_{max} = 0.44 kN. Then, some new mode I fatigue cracks occurred. However, we stopped the test at $N = 1.0 \times 10^7$ because the crack was arrested again. Moreover, the crack in the hybrid specimen with the reversed setting was arrested. Meanwhile, the normal specimen failed at $N = 4.0 \times 10^5$. We found a major difference in the crack growth rate between the specimens with and without the interleaf. We measured a as the largest in the case of observable crack tips on the interface of the hybrid specimen with P_{max} = 0.44 kN because the crack on the surface occurred intermittently.

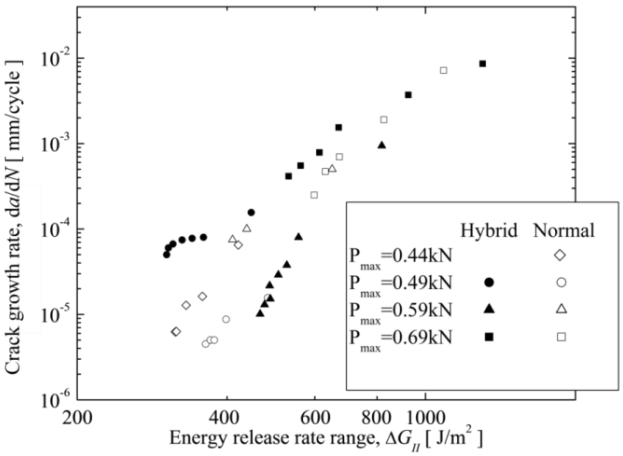

Figure 5. Relation between crack growth rate and energy release rate range.

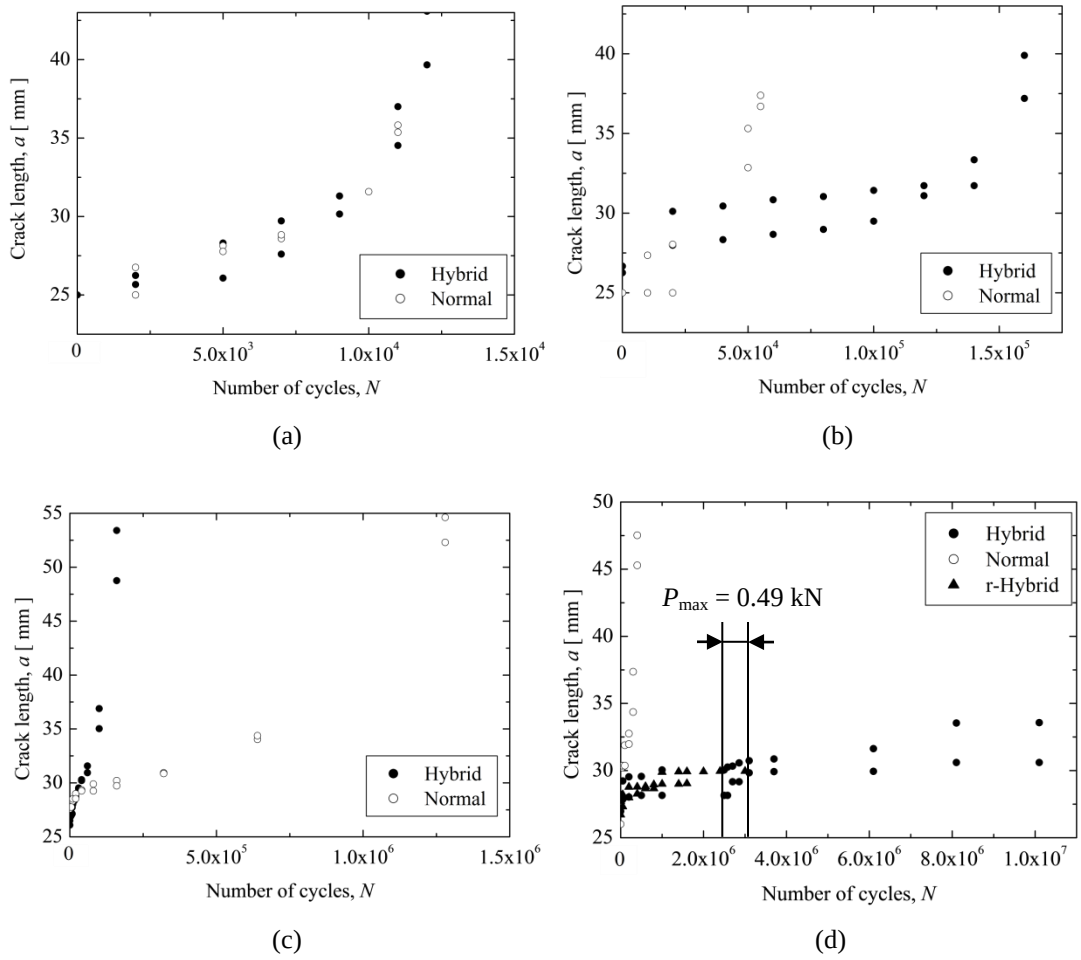

Figure 6. Relation between crack length and number of cycles under maximum load:
(a) 0.69 kN, (b) 0.59 kN, (c) 0.49 kN, (d) 0.44 kN.

4 Discussion

The scattering in the medium load region is described. The crack growth rate at P_{max} = 0.59 kN was less than that at P_{max} = 0.49 kN. We did not find a difference between the surfaces. Accordingly, we observed the fatigue fracture surface of the hybrid specimens. Figure 7(a-h) and (b-h) shows the fracture surface at P_{max} = 0.59 kN and 0.49 kN, respectively. We found that the number of fibers and glass debris in Fig. 7(b-h) was more than that in Fig. 7(a-h). Glass debris occurred because fibers were damaged by friction. This indicates that the fatigue crack at P_{max} = 0.59 kN grew along the interface between the interleaf and the UD layer, and the fatigue crack at P_{max} = 0.49 kN grew between the UD layers. Hojo et al. [7] reported that carbon fiber (CF)/epoxy laminates with self-same epoxy interleaf showed increased mode II interlaminar properties. The same thing occurred at P_{max} = 0.59 kN, so the crack growth rate at P_{max} = 0.59 kN was less than that at P_{max} = 0.49 kN. The crack path appeared to be related to the degree of resin impregnation. Next, the crack growth rate at P_{max} = 0.49 kN was less than that at P_{max} = 0.44 kN. Figure 8(a-n) and (b-n) shows the side surface of the normal specimens at P_{max} = 0.49 kN and 0.44 kN, respectively. The state of the lamination of the UD layers at P_{max} = 0.44 kN was worse than that at P_{max} = 0.49 kN. This is why the crack growth rate at P_{max} = 0.49 kN was less than that at P_{max} = 0.44 kN. That was the reason for the scattering in the medium load region. An improvement in laminate manufacturing methods is necessary to prevent this scattering.

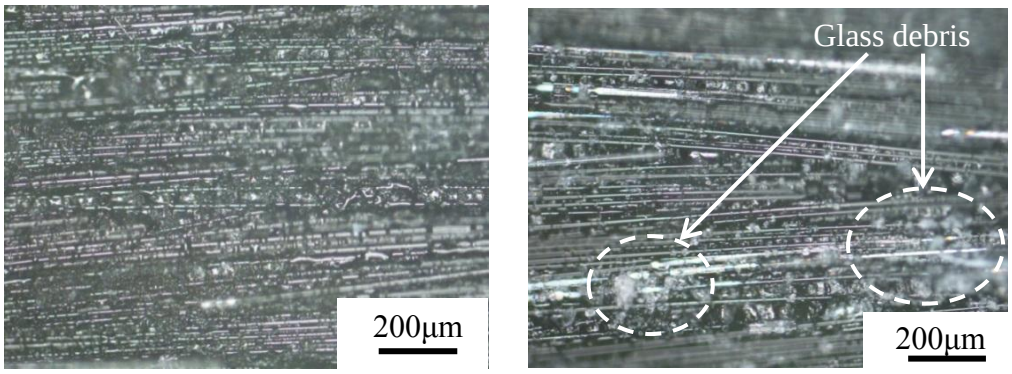

(a-h) (b-h)

Figure 7. Mode II fatigue fracture surfaces of hybrid laminates at a = 33 mm in
(a-h) P_{max} = 0.59 kN (N = 1.42 × 10^5, ΔG_{II} = 578 J/m^2);
(b-h) P_{max} = 0.49 kN (N = 7.87 × 10^4, ΔG_{II} = 400 J/m^2).

(a-n)

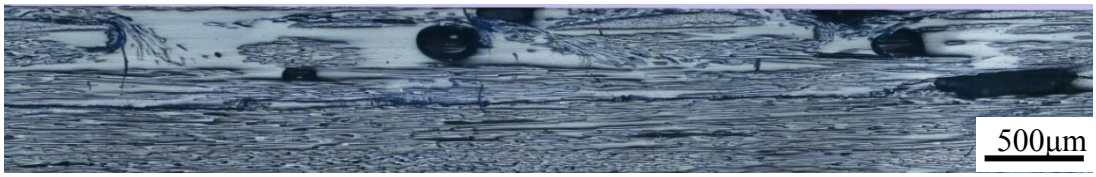

(b-n)

Figure 8. Side surfaces of normal laminates at a = 33.5 mm in
(a-N) P_{max} = 0.49 kN (N = 2.52 × 10^5, ΔG_{II} = 464.4 J/m^2);
(b-N) P_{max} = 0.44 kN (N = 1.33 × 10^5, ΔG_{II} = 377.8 J/m^2).

Figure 9 shows the side surface of the hybrid specimen with the usual setting at P_{max} = 0.44 kN. This crack growth behavior is very different from the others. More specifically, some mode I fatigue cracks were caused by principal stress. In addition, short fibers and resin debris were observed in the interleaf, around the crack. This indicates that the interleaf was damaged by fracture surface wearing. Figure 10 shows the side surface of the hybrid specimen with the reversed setting at P_{max} = 0.44 kN. Some mode I fatigue cracks, short fibers, and resin debris were observed. The crack growth behavior appeared to be the same as that of the hybrid specimen with the usual setting. Accordingly, for P_{max} = 0.44 kN, the fatigue crack growth rate was decreased by the occurrence of mode I cracks and wear in the interleaf.
Crack prevention due to the interleaf was observed at P_{max} = 0.44 kN, which was the lowest load used in this study. The interleaf appeared to be effective for crack prevention in a region of relatively low energy release rate. However, a definite condition for crack prevention was not clear. We assume that further studies will be conducted under various test conditions.

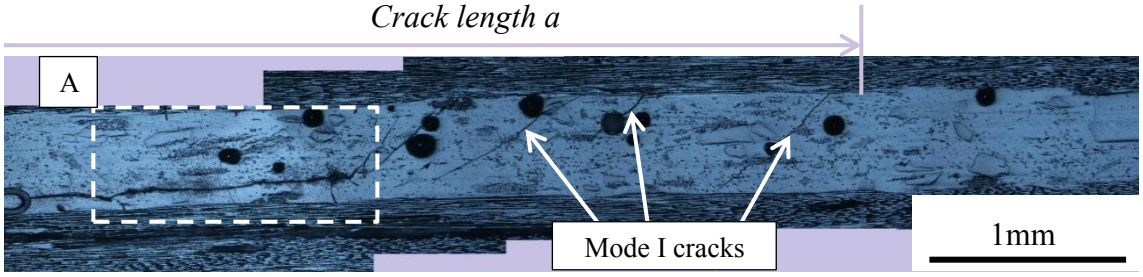

(a)

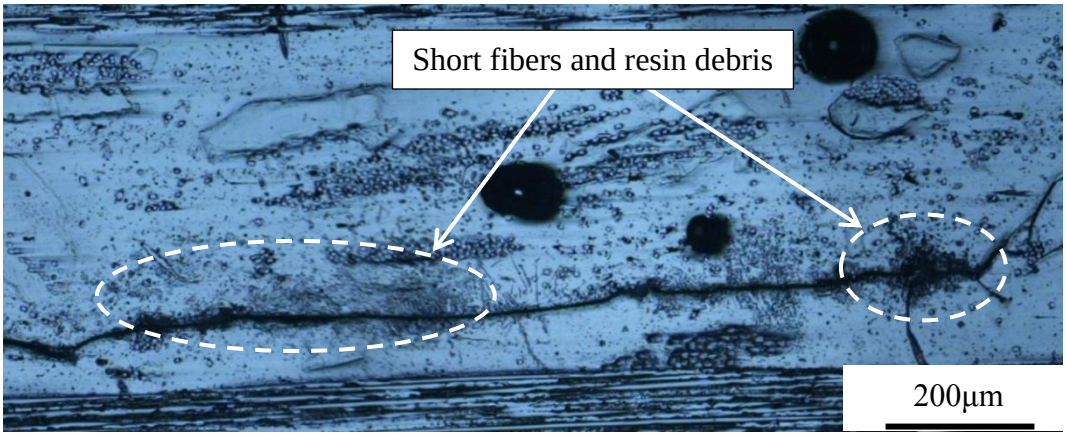

(b)

Figure 9. Side surface of hybrid laminates at P_{max} = 0.44 kN:
(a) the whole figure; (b) the detail of A. (a = 32 mm, N = 8.1 × 10^6, usual setting).

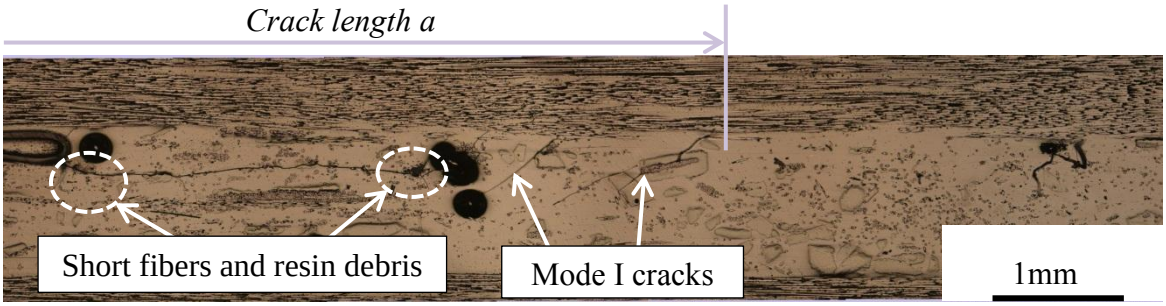

Figure 10. Side surface of hybrid laminates at P_{max} = 0.44 kN
(a = 30 mm, N = 3.0 × 10^6, reverse setting).

5 Conclusions

We determined the mode II delamination fatigue crack growth characteristics of GFRP laminates with an interleaf comprising waste GFRP milled chips. The interleaf was effective in impeding crack growth in a region with a relatively low energy release rate.

References

[1] Aono Y., Murae S., Kubo T. Static Mechanical Properties of GFRP Laminates with Waste GFRP Interleaf. *Procedia Engineering*, **10**, pp. 2080-2085 (2011).

[2] Lee S.H., Noguchi H., Kim Y.B., Cheong S.K. Effect of Interleaved Non-Woven Carbon Tissue on Interlaminar Fracture Toughness of Laminated Composites. *Journal of Composite Materials*, **36**, pp. 2153-2182 (2002).

[3] Matsubara G., Ono H., Tanaka K. Mode II Fatigue Crack Growth from Delamination in Unidirectional Tape and Satin-woven Fabric Laminates of High Strength GFRP. *International Journal of Fatigue*, **28**, pp. 1177-1186 (2006).

[4] Shindo Y., Takeda T., Narita F., Saito N., Watanabe S., Sanada K. Delamination Growth Mechanisms in Woven Glass Fiber Reinforced Polymer Composites under Mode II Fatigue Loading at Cryogenic Temperatures. *Composites Science and Technology*, **69**, pp. 1904-1911 (2009).

[5] Schön J. A Model of Fatigue Delamination in Composites. *Composites Science and Technology*, **60**, pp. 553-558 (2000).

[6] Matsuda S., Hojo M., Ochiai S. Mesoscopic Fracture Mechanism of Mode II Delamination Fatigue Crack Propagation in Interlayer-Toughened CFRP. *JSME international journal. Series A, Solid Mechanics and Material Engineering*, **40**, pp. 423-429 (1997).

[7] Hojo M., Ando T., Tanaka M., Adachi T., Ochiai S., Endo Y. Modes I and II Interlaminar Fracture Toughness and Fatigue Delamination of CF/epoxy Laminates with Self-Same Epoxy Interleaf. *International Journal of Fatigue*, **28**, pp. 1154-1165 (2006).